Modelling neurotransmitter functions: a laser spectroscopic study of (1*S*,2*S*)-*N*-methyl pseudoephedrine and its complexes with achiral and chiral molecules

A. Giardini Guidoni,[a,b] A. Paladini,[a,b] S. Piccirillo,*[c] F. Rondino,[a] M. Satta[d] and M. Speranza*[e]

Received 20th February 2006, Accepted 17th March 2006
First published as an Advance Article on the web 11th April 2006
DOI: 10.1039/b602510b

Wavelength and mass resolved resonance-enhanced two photon ionization (R2PI) excitation spectra of (1*S*,2*S*)-*N*-methyl pseudoephedrine (**MPE**) and its complexes with several achiral and chiral solvent molecules, including water (**W**), methyl (*R*)-lactate ($\mathbf{L_R}$), methyl (*S*)-lactate ($\mathbf{L_S}$), (*R*)-2-butanol ($\mathbf{B_R}$), and (*S*)-2-butanol ($\mathbf{B_S}$), have been recorded after a supersonic molecular beam expansion and examined in the light of *ab initio* calculations. The spectral patterns of the selected complexes have been interpreted in terms of the specific hydrogen-bond interactions operating in the diastereomeric complexes, whose nature in turn depends on the structure and the configuration of the solvent molecule. The obtained results confirm the view that a representative neurotransmitter molecule, like **MPE**, "communicates" with the enantiomers of a chiral substrate through different, specific interactions. These findings can be regarded as a further contribution to modelling neurotransmitter functions in biological systems.

Introduction

The last few years have witnessed a tremendous development in molecular biology with the deciphering of the human genome and its implications into the search of new personalized treatments. This pharmacogenetic programme, which aims to design new drugs adapted to each human being, requires sophisticated modelling of biomolecules as well as understanding the biochemical mechanism at the molecular level. Although impressive developments have been made along this direction, some fundamental aspects, such as the detailed mechanism of molecular recognition and, particularly, reaction dynamics are not well understood. Biomolecules are often chiral and many biochemical processes show preference for one enantiomer over the other. Recognition of a chiral drug by a suitable chiral receptor, which is the basis of its biological activity (including pharmacology and toxicology), involves size- and shape-specific non-covalent interactions, such as van der Waals, electrostatic, or hydrogen bonding attractions tempered by steric repulsions. Detailed comprehension of these forces is crucial for understanding, on a molecular level, the principles that govern chiral recognition and, therefore, for targeting drugs to specific receptors. Besides, modelling drug activity requires the study of tailor-made simplified host/guest systems under conditions mimicking the extensive desolvation of the biomolecule when entering the receptor cavity, *i.e.* in the gas phase.

In recent years, a number of laser REMPI and LIF spectroscopic studies on the structure, dynamics, and reactivity of diastereomeric complexes between chiral molecules, *e.g.* alcohols and amines, and suitable chiral receptors have been carried out by us[1–4] and others.[5–8] These studies provided precious information on the conformational changes of the chiral components by aggregation as well as on the nature of the intervening non-covalent forces. Some of these studies regarded the simplest members of the class of neurotransmitters as amphetamine, dopamine, noradrenaline, ephedrine and others. The $S_1 \leftarrow S_0$ transition origins of their various conformers have been recorded and their structures determined with the help of *ab initio* calculations.[9–14] An important aspect of these studies concerns the conformational changes of the neurotransmitter molecule by monosolvation. No information is available to date as regards to the van der Waals and hydrogen-bond interactions between a chiral solvent molecule and a neurotransmitter, which represents the basis of the receptor chiral recognition of a neurotransmitter molecule. A first insight into this point is provided in this paper, which reports on the results of a one color R2PI-TOF spectroscopic study of a specific neurotrasmitter molecule, *i.e.* (1*S*,2*S*)-*N*-methyl pseudoephedrine (**MPE**), involved in neuronal communication. Its behaviour is compared with that of other neurotransmitters, like ephedrine and pseudoephedrine. The effects of **MPE** monosolvation by water (**W**), (*R*)-2-butanol ($\mathbf{B_R}$), (*S*)-2-butanol ($\mathbf{B_S}$), methyl (*R*)-lactate ($\mathbf{L_R}$), and methyl (*S*)-lactate ($\mathbf{L_S}$) have been investigated as well. It is hoped thereby to provide a comparative picture of the monosolvation effects of these important molecules and some fundamental information of the forces governing their chiral recognition by receptor mimics.

[a]*Dipartimento di Chimica, Università di Roma "La Sapienza", pl. A. Moro 5, I-00185, Roma, Italy*
[b]*CNR-IMIP (sezione Istituto Materiali Speciali), I-85050, Tito Scalo (Pz), Italy*
[c]*Università di Roma "Tor Vergata", Dipartimento di Scienze e Tecnologie Chimiche, Via della Ricerca Scientifica, I-00133, Rome, Italy. E-mail: piccirillo@fisica.uniroma2.it; Tel: +39-06-72594400*
[d]*CNR-ISC (Istituto dei Sistemi Complessi), I-00185, Roma, Italy*
[e]*Facoltà di Farmacia, Dipartimento di Studi di Chimica e Tecnologia delle Sostanze Biologicamente Attive, Università di Roma "La Sapienza", pl. A. Moro 5, I-00185, Roma, Italy. E-mail: maurizio.speranza@uniroma1.it; Fax: +39-06-49913602; Tel: +39-06-49913497*

Experimental

R2PI-TOF experiments

The experimental set up to produce the molecular clusters and to perform their spectral analysis has been described elsewhere.[15,16] The supersonic beam of the species of interest was obtained by adiabatic expansion of a carrier gas (Ar; stagnation pressure from 2 to 4 bar), seeded with (1*S*,2*S*)-*N*-methyl pseudoephedrine (**MPE**) and different solvents through a heated pulsed nozzle of 400 μm i.d (aperture time: 200 μs; repetition rate: 10 Hz) heated at $T = 100$ °C. Their concentration is maintained enough low to minimise the production of heavier clusters. The molecular beam was allowed to pass through a 1-mm diameter skimmer into a second chamber equipped with a vertical TOF spectrometer. Molecules and clusters in the beam are excited and ionised by one or two tuneable dye lasers, pumped by a Nd:YAG laser ($\lambda = 532$ nm). The dye fundamental frequencies are doubled and, when necessary, mixed with residual 1064 nm radiation to obtain two different frequencies ν_1 and ν_2. The ions formed by R2PI ionizations are mass discriminated and detected by a channeltron after a 50-cm flight path. The mass selected ionic signals are recorded and averaged by a digital oscilloscope and stored on a PC.

One-colour R2PI experiments (1cR2PI) involve electronic excitation of the species of interest by absorption of one photon $h\nu_1$ and by its ionisation by a second photon of the same energy $h\nu_1$. The 1cR2PI excitation spectra were obtained by recording the entire TOF mass spectrum as a function of ν_1. The wavelength dependence of a given mass resolved ion represents the absorption spectrum of the species and contains important information about its electronic excited state S_1.

Computational details

MM3 force-field classical molecular dynamics is run for each neutral adduct at a temperature of 800 K with some constraints to overcome dissociation; the cumulative time is 0.1 ns with a time step of 0.5 fs and a dump time of 1 ps. The 100 snapshots are then optimized with a convergence of 10^{-6} kcal mol^{-1} Å^{-1} RMS gradient per atom. The obtained optimized structures are classified according to their energy and conformation.

The **MPE** molecule and the [**MPE·W**] clusters have been studied by DFT approach: we used the B3LYP Hamiltonian with the 6-31G** basis set for both energy and geometrical optimization. Each [$\mathbf{MPE{\cdot}L_{R/S}}$] and [$\mathbf{MPE{\cdot}B_{R/S}}$] cluster conformer is optimized with a Hartree–Fock approach using a medium size basis set. The convergence criterion for energy calculations is 10^{-6} Hartrees. The basis set is the 6-31G. The ionization potentials have been estimated using the semiempirical PM3 Hamiltonian. All the *ab initio* calculations were performed using the GAUSSIAN 98 package.[17] Vibrational frequencies were calculated using the B3LYP density functional method and a 6-31G** basis set, previously found to give fair agreement with experimental data for similar molecules[18–19] when scaling factors of 0.97 are used.

Results and discussion

The bare MPE molecule

Ab initio B3LYP/6-31G** calculations point to the existence of two stable conformers for the isolated **MPE** molecule, *i.e.* **MPE1** and **MPE2** (Fig. 1). The **MPE1** conformer presents an intramolecular OH···N hydrogen bond, while the **MPE2** is characterized by the presence of the OH group pointing towards the π ring. Accordingly, **MPE2** was found to lie 6.5 kcal mol^{-1} above **MPE1**, which is therefore the global minimum. As a consequence, it is very likely that supersonic expansion of (1*S*,2*S*)-*N*-methyl pseudoephedrine yields predominantly, if not exclusively, the most stable **MPE1** conformer.

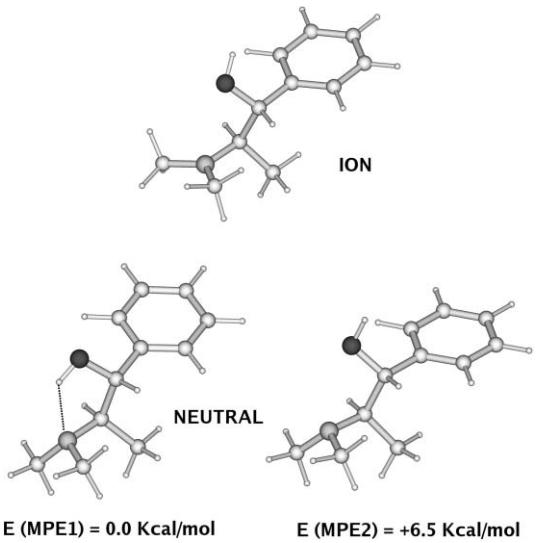

Fig. 1 *Ab initio* B3LYP/6-31G** most stable structures for the isolated neutral **MPE** molecule and PM3 geometry for the ion. The figure reports also the calculated energies.

Fig. 1 reports the PM3-calculated structure of the corresponding radical ion as well. The ionization potentials of **MPE1** and **MPE2** are calculated as large as 7.52 and 7.45 eV, respectively. A common behaviour of photoionized ephedrine and pseudoephedrine is that of undergoing extensive breaking of their C_α–C_β bond to give the corresponding $[CH_3CHNHCH_3]^+$ fragment (m/z 58).[10,13] A similar fragmentation is even more extensive in **MPE** (>99%) to give the fragment at m/z 72, *i.e.* $[CH_3CHN(CH_3)_2]^+$. This behavior is favored by the presence of an extra-methyl at the N center, resulting in an extra-stabilization of the positive charge of the fragment. Another major factor determining the almost complete [**MPE**]$^+$ fragmentation is the large excess of energy ($\Delta E = E_{hv} - IP \approx 1.8$ eV), imparted to the molecule by absorption of two photon during the 1cR2PI process ($E_{hv} = 9.3$ eV). This excess energy is probably enough to overcome the barrier to fragmentation, if actually present.[20] Important geometry changes occur in the monomer upon ionization. Frank–Condon factors leave the molecular cation in highly excited vibrational states leading to rapid fragmentation.

The 1cR2PI-TOF absorption spectrum of the isolated **MPE** molecule, recorded at m/z 72, is illustrated in Fig. 2. A strong feature at 37578 cm^{-1} is observed which can be assigned to the 0_0^0 electronic $S_1 \leftarrow S_0$ transition of the most stable conformer **MPE1**. A much weaker peak at 37535 cm^{-1} can also be identified as the 0_0^0 electronic $S_1 \leftarrow S_0$ transition and attributed to the less stable conformer **MPE2**. On the basis of pressure studies, the other two peaks red shifted with respect to the 37578 cm^{-1} have been attributed to larger clusters fragmenting to the m/z 72 mass

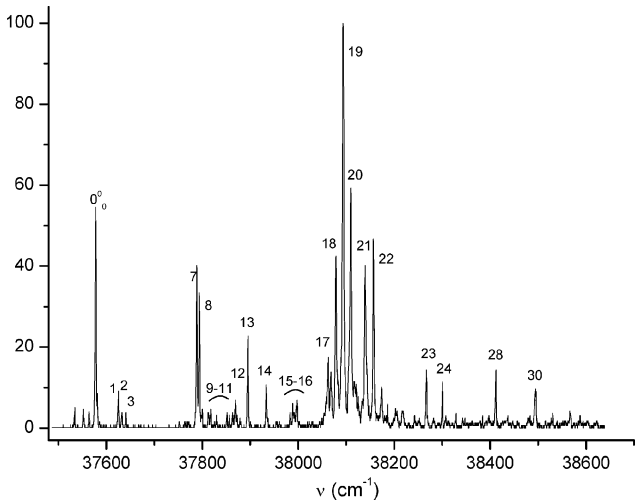

Fig. 2 1cR2PI Excitation spectrum of the isolated molecule (1*S*,2*S*)-methylpseudoephedrine (**MPE**) measured at $m/z = 72$. The main vibronic bands, characteristic of the spectra of substituted benzenes, are marked in the spectrum (see Table I).

channel. This observation fully conforms to the theoretical estimate of the relative stability of the two conformers. The excitation spectrum in the frequency range from 37500 to 38600 cm^{-1} (Fig. 2) is characterized by a set of bands blue shifted with respect to the 0_0^0 electronic $S_1 \leftarrow S_0$ transition at 37578 cm^{-1} which can be assigned to the vibronic transitions of the most stable conformer **MPE1** (Table 1). Some of the minor peaks can be attributed to the vibration of the less populated conformer **MPE2**. The vibronic transitions have been tentatively assigned by comparing the experimental peaks of Fig. 2, representative of the vibrational modes of **MPE1** in the S_1 excited state, with: (i) those computed at B3LYP/6-31G** level of theory in harmonic approximation for **MPE1** in the S_0 ground state (Table 1); and (ii) with experimental data from related alkylaromatic systems.[2,19,21]

The not intense vibronic bands labelled 1,2 and 3, blue shifted relative to the 0_0^0 band origin of **MPE1** by 47, 55 and 63 cm^{-1}, respectively, are assigned to torsions of the molecule. The quite intense bands marked 7 and 8, respectively at 211 and 216 cm^{-1}, are assigned to the in plane bending and rocking. The tentative assignments of the other bands can be found in Table 1.

The [MPE·W] complex

Fig. 3 reports the B3LYP/6-31G** optimized structures of the three most stable clusters between **MPE** and one water (**W**) molecule. The relevant binding energies and ionization potentials are listed in Table 2. The most stable isomer α is characterized by a structure similar to **MPE1** with its O center acting as proton acceptor from **W** and as proton donor to the amino group. In the second most stable isomer β, the **W** molecule is inserted into the two functionalities of **MPE** and acts as proton acceptor from the OH group of the chromophore and as proton donor to its N center. In the least stable conformer γ, this latter interaction is prevented by the unfavorable C_α–OH bond orientation.

The 1cR2PI-TOF absorption spectra of the [**MPE·W**] complex, taken at m/z 179 ([**MPE**]$^+$), m/z 90 ([$CH_3CHN(CH_3)_2$·**W**]$^+$), and m/z 72 ([$CH_3CHN(CH_3)_2$]$^+$) are shown in Fig. 4a–c, respectively. All of them exhibit several bands (marked with asterisks in

Table 1 Calculated vibrational frequencies ν_{th} for the S_0 ground state of **MPE1**. Measured vibrational frequencies ν_{exp} for the S_1 excited state of **MPE1**

Band number[a]	Modes	S_0 state MPE1 ν_{th}/cm^{-1}	S_1 state MPE1 ν_{exp}/cm^{-1}
	0_0^0	0	0
1	C_α–C_β torsion, C_β–C_γ torsion	42	47
2	C_β–C_γ torsion	54	55
3	C_γ–N torsion	75	63
7	Rocking (CH_3)	225	211
8	Rocking (CH_3)	231	216
9	Rocking (CH_3), out of plane bending plane C_α–C_β	242	220–288
10	Rocking (CH_3)	256	
11	Rocking (CH_3)	277	
12	CH_3 torsion	283	292
13	Bending C_α–C_β–O, ring bending in plane	352	317
14	Butterfly ring	401	355
15	N-umbrella	412	404–420
16	Bending CH_3–N–CH_3, butterfly ring	422	
17	Bending C_α–C_β–N, bending CH_3–N–C_γ	498	484
18	Butterfly ring	526	501
19	Bending C_α–C_β–N, bending O–C_α–C_β	545	515
20	Asymmetric ring breathing	609	531
21	Symmetric ring breathing, bending O–C_α–C_β	614	562
22	H–O–C_β–C_γ torsion	644	579
23	Butterfly ring	688	689
24	Out of plane bending	730	723
28	Stretching C_α–C_β, CH_3 bending	857	834
30	CH_3 bending	933	918

[a] Band numbering as reported in Fig. 2.

Table 2 Calculated binding energies (D'') and ionization potentials (IP) of the three conformers of [MPE·W]. D''_e is the uncorrected binding energy, $^{BSSE}D''_e$ is the binding energy corrected for the basis set superposition error and $^{BSSE}D''_0$ is corrected also for the zero point vibrational frequencies

Conformer	Relative total energy/kcal mol^{-1}	Binding energy/kcal mol^{-1} [a]			IP/eV[b]
		D''_e	$^{BSSE}D''_e$	$^{BSSE}D''_0$	
α	0.0	10.3	4.8	2.3	8.0
β	1.5	15.5	8.2	5.6	7.4
γ	6.7	8.9	5.1	3.0	7.3

[a] B3LYP/6-31G**; [b] PM3.

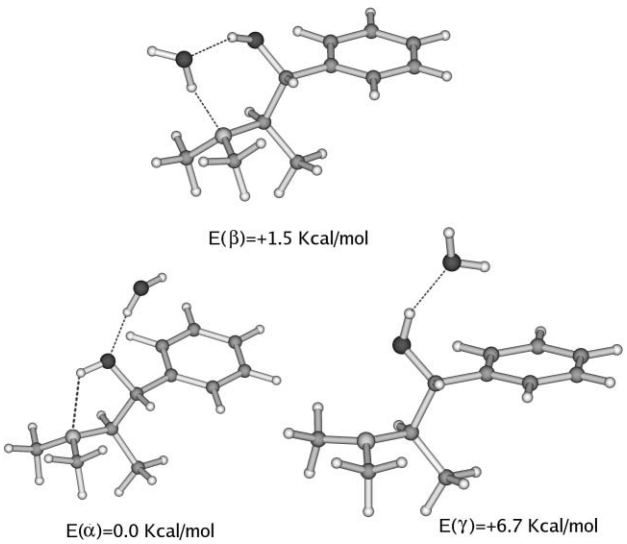

Fig. 3 *Ab initio* B3LYP/6-31G** most stable structures and predicted energies for the [**MPE·W**] complex.

Fig. 4a–c), one intense at 37595 cm^{-1} and other more intense at 37581 cm^{-1}, both blue-shifted relative to the $S_1 \leftarrow S_0$ band of the bare **MPE1** chromophore (37578 cm^{-1}, broken line in Fig. 4) by $\Delta\nu = +17$ and $+3$ cm^{-1}, respectively. The close similarity of the spectra, taken m/z 179 and 72, with that taken at m/z 90 ([$CH_3CHN(CH_3)_2$·**W**]$^+$) points to these fragments as all originating from the [**MPE·W**]$^+$ complex (eqn 1–3). In this frame, the observation of relatively abundant [**MPE**]$^+$ fragments (m/z 179) from [**MPE·W**]$^+$, otherwise almost undetectable from bare **MPE1**, suggests that monohydration of **MPE1**, besides leading to the blue-shifting of the $S_1 \leftarrow S_0$ band origin of the chromophore, appreciably increases its IP. On the grounds of the computed IP's of Table 2, one is inclined to assign structure α of Fig. 3 to most of the supersonically expanded [**MPE·W**]$^+$ complexes.

$$[\mathbf{MPE{\cdot}W}]^{+\cdot} \rightarrow [\mathbf{MPE}]^{+\cdot} + \mathbf{W} \quad (1)$$

$$[\mathbf{MPE{\cdot}W}]^{+\cdot} \rightarrow [CH_3CHN(CH_3)_2{\cdot}\mathbf{W}]^{+} + PhCHOH^{\cdot} \quad (2)$$

$$[\mathbf{MPE{\cdot}W}]^{+\cdot} \rightarrow [CH_3CHN(CH_3)_2]^{+} + PhCHOH^{\cdot} + \mathbf{W} \quad (3)$$

The diastereomeric [MPE·$L_{R/S}$] complexes

A similar behaviour is observed in the case of the complexes of **MPE** with methyl lactates $\mathbf{L_R}$ and $\mathbf{L_S}$. The calculations performed on the corresponding complexes have been focused on the most stable conformers identified by molecular dynamics

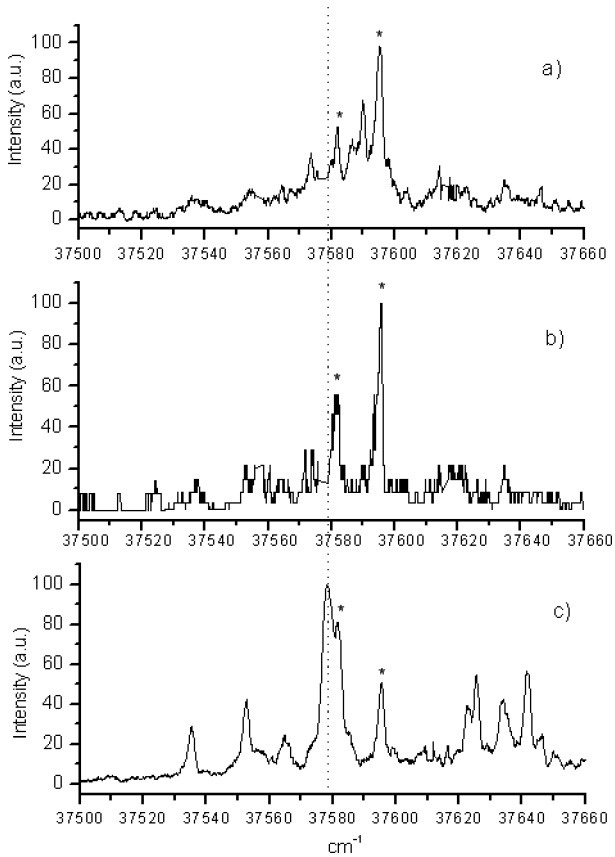

Fig. 4 1cR2PI Excitation spectra obtained by monitoring the [**MPE·W**] complex at $m/e = 179$ (a), m/e = 90 (b), and m/e = 72 (c).

simulations. Seven *ab initio* HF/6-31G-optimized structures have been identified for each of the two diastereomeric [**MPE·$\mathbf{L_{R/S}}$**] forms with energy differences not exceeding 10 kcal mol^{-1} (Fig. 5). Inspection of the figure reveals that there is a close correspondence between the structure and the energy of the most stable homo- and the heterochiral adducts. In fact, the above structures have almost the same relative energies and geometries except for the interchange in the position of a methyl group with an hydrogen atom. The two most stable conformers (A and B of Fig. 5) are analogous to structure α of the [**MPE·W**] complex with the O of the chromophore acting as proton acceptor from $\mathbf{L_{R/S}}$ and as proton donor to the amino group. Similar interactions operate in the less stable structure D ($\Delta E = 3.3$–3.4 kcal mol^{-1}). The insertion complex C ($\Delta E = 2.6$–2.9 kcal mol^{-1}) presents close analogies with structure β of the [**MPE·W**] complex with the OH group of $\mathbf{L_{R/S}}$ molecule acting as proton acceptor from the OH group of the

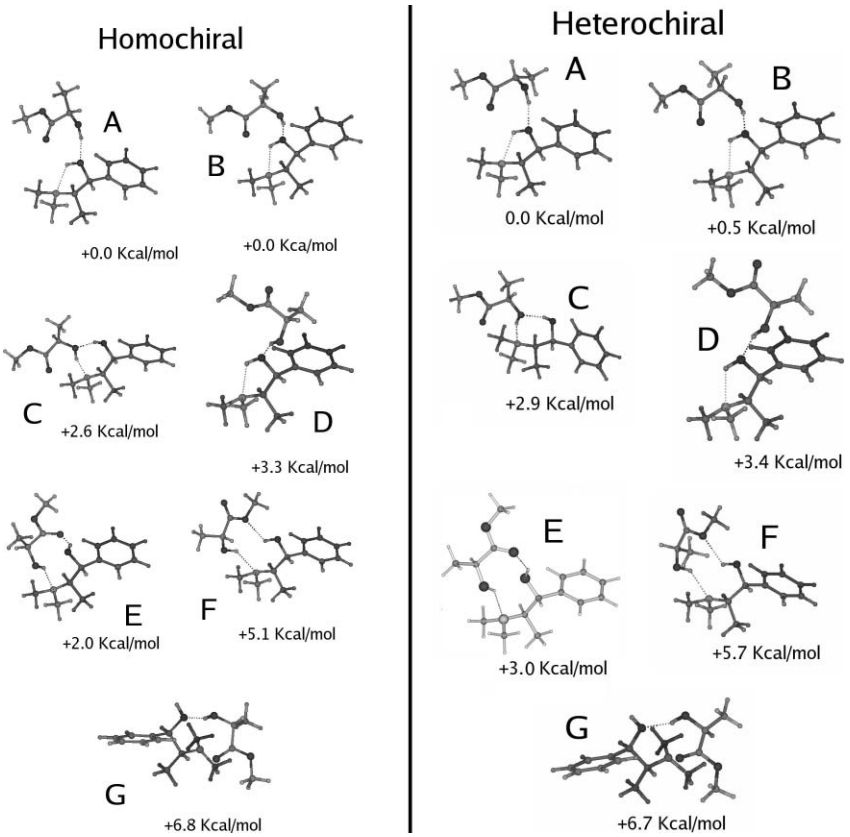

Fig. 5 *Ab initio* HF/6-31G most stable structures and predicted energies for the homochiral [**MPE·L**$_S$] and heterochiral [**MPE·L**$_R$] complexes.

chromophore and as proton donor to its N center. The least stable G isomers of the [**MPE·L**$_{R/S}$] complexes ($\Delta E = 6.7$–6.8 kcal mol^{-1}) are structurally similar to form γ of the [**MPE·W**] complex with the OH group of the chromophore acting exclusively as proton acceptor from the OH group of the **L**$_{R/S}$ molecule. The presence of the methoxycarbonyl function adjacent to the OH one in **L**$_{R/S}$ allows the formation of additional isomers where the carbonylic oxygen of **L**$_{R/S}$ acts as a proton acceptor from the OH of the chromophore while its OH group interacts with the N center of the **MPE** (structures E in Fig. 5; $\Delta E = 2.0$–3.0 kcal mol^{-1}). In the slightly less stable isomers F ($\Delta E = 5.1$–5.7 kcal mol^{-1}), the same interactions involve the ethereal oxygen instead of the carbonyl oxygen. In both the D and F structures the lactate has the OH group "*trans*" in respect to its C=O group, whereas in all the other conformers the OH group is "*cis*" to the C=O group, that corresponds to the more stable conformation of the free lactate.

The 1cR2PI-TOF mass spectra of the diastereomeric [**MPE·L**$_{R/S}$] complexes are characterized by their complete C_α–C_β fragmentation accompanied by the loss of the **L**$_{R/S}$ molecule. Their 1cR2PI-TOF absorption spectra, taken at m/z 72 ($[CH_3CHN(CH_3)_2]^+$), are shown in Fig. 6a–b. Relative to the spectral features of the bare **MPE1** chromophore, the spectral patterns of the diastereomeric [**MPE·L**$_{R/S}$] complexes are characterized by the presence of new red-shifted bands (marked with asterisks in Fig. 6). The heterochiral complex exhibits only a single red-shifted peak ($\Delta\nu = -158$ cm^{-1}; Fig. 6a), whereas the homochiral one display two red-shifted bands ($\Delta\nu = -174$ and -144 cm^{-1}; Fig. 6b). It is worth noting that the red-shifted peak

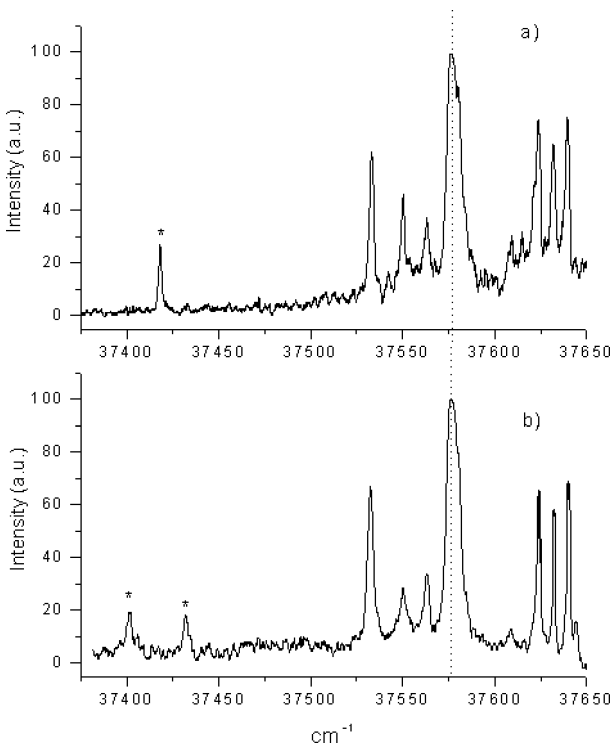

Fig. 6 1cR2PI Absorption spectrum of the **MPE** complex with methyl (*R*)-(+)-lactate **L**$_R$ (a) and methyl (*S*)-(−)-lactate **L**$_S$ (b) obtained by monitoring the fragment ion signals at $m/e = 72$.

of the heterochiral complex falls just halfway the frequency gap between the two red-shifted bands the homochiral adduct ($\Delta\nu$ = 30 cm^{-1}). A similar situation has been already observed for other diastereomeric clusters.[22–24] It is tempting to attribute the two red-shifted bands of the homochiral adduct to the most stable degenerate A and B rotamers (Fig. 5). Analogously, the single red-shifted signal of the heterochiral complex is associated with the most stable A conformer, while the slightly less stable structure B may not be sufficiently abundant at the low temperatures typical of supersonically expanded beams to produce a detectable signal.

The diastereomeric [MPE·$B_{R/S}$] complexes

The diastereomeric [**MPE**·$\mathbf{B_{R/S}}$] complexes behave in conformity with the analogous [**MPE**·$\mathbf{L_{R/S}}$] and [**MPE**·**W**] ones. Fig. 7 reports the HF/6-31G optimized structures of the three most stable [**MPE**·$\mathbf{B_{R/S}}$] structures. In particular, the most stable isomers **I** and **II** present an intramolecular OH···N and an intermolecular OH···O interaction in which the $\mathbf{B_{R/S}}$ acts as a proton donor to **MPE**. In the second most stable isomers **III** and **IV**, the $\mathbf{B_{R/S}}$ molecules act as proton acceptor from the OH group of the chromophore and as proton donor to its N center. The least stable structures **V** and **VI** are instead characterized by a bifurcated H-bond between the OH group of the chromophore acting as proton donor to both its N center and the OH group of $\mathbf{B_{R/S}}$.

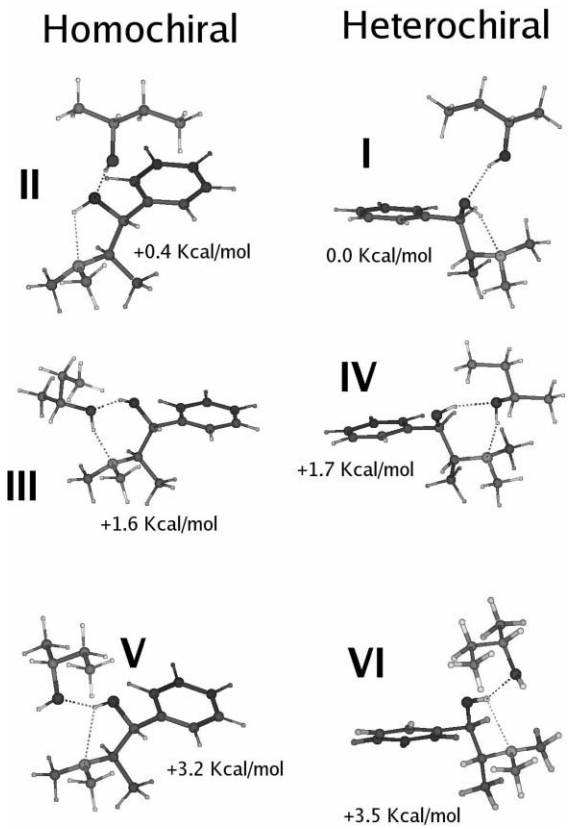

Fig. 7 *Ab initio* HF/6-31G most stable structures and predicted energies for the homochiral [**MPE**·$\mathbf{B_s}$] and heterochiral [**MPE**·$\mathbf{B_R}$] complexes.

The 1cR2PI-TOF mass spectrum of the homochiral [**MPE**·$\mathbf{B_S}$] complex is characterized by the formation of small yields of the $[CH_3CHN(CH_3)_2]^+$ fragment (m/z 72), together with minor amounts of the [**MPE**]$^+$ (m/z 179) and $[CH_3CHN(CH_3)_2\cdot\mathbf{B_S}]^+$ (m/z 146) ones (refer to eqn 1–3). Very minor quantities of the intact [**MPE**·$\mathbf{B_S}$]$^+$ complex are observable as well (Fig. 8). The intensity of these peaks does not allow a sufficiently accurate analysis of the relevant 1cR2PI-TOF absorption spectra. However, the spectra qualitatively show the same general features of the [**MPE**·$\mathbf{L_{R/S}}$] and [**MPE**·**W**] ones, *i.e.* few bands red-shifted by a given $\Delta\nu$ value relative to the $S_1 \leftarrow S_0$ band of the bare **MPE1** chromophore by the same $\Delta\nu$ values. Concerning the heterochiral [**MPE**·$\mathbf{B_R}$] complex, no signs of the presence of the m/z 72, 146, 179, and 253 fragments are observed. This lack of signals is attributed to the complete fragmentation of the heterochiral complex to give the m/z 72 one, whose intensity is so low to make it indistinguishable from the intense m/z 72 fragments arising from the bare **MPE1** molecule.

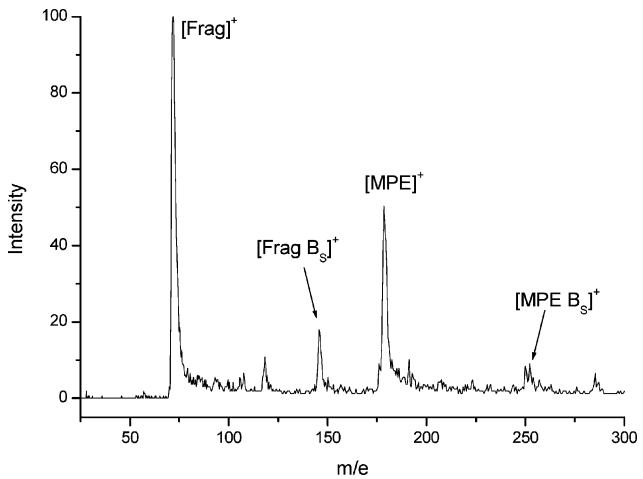

Fig. 8 1cR2PI Mass spectrum of the **MPE**/(*S*)-2-butanol $\mathbf{B_S}$ mixture. The spectrum is taken at ν = 37560 cm^{-1}.

Conclusions

The present study shows how R2PI-TOF spectroscopy coupled with high level *ab initio* calculations can provide valuable insights into the properties of a representative neurotransmitter molecule. Important aspects of molecular shape and interaction forces between **MPE** and few chiral and achiral solvent molecules can be inferred from the analysis of the mass resolved excitation spectra. In the [**MPE**·**W**] cluster, different structures leading to peculiar fragmentation are identified. In particular, water appears to bind the OH and the NH group of the chromophore in different ways leading to different conformers. A similar situation is found with the diastereomeric [**MPE**·$\mathbf{L_{R/S}}$] and [**MPE**·$\mathbf{B_{R/S}}$] pairs. Here, the chiral **MPE** chromophore is able to enantiodifferentiate the selected chiral molecules on the grounds of a subtle interplay between the difference in the van der Waals forces operating in the corresponding diastereomeric aggregates.

Acknowledgements

Contract grant sponsors: Ministero della Università e della Ricerca Scientifica e Tecnologica (MURST-COFIN) and Consiglio Nazionale delle Ricerche (CNR).

References

1 A. Latini, D. Toja, A. Giardini Guidoni, A. Palleschi, S. Piccirillo and M. Speranza, *Chirality*, 1999, **11**, 376.
2 A. Giardini Guidoni, S. Piccirillo, D. Scuderi, M. Satta, T. M. Di Palma and M. Speranza, *Phys. Chem. Chem. Phys.*, 2000, **2**, 4139.
3 D. Scuderi, A. Paladini, S. Piccirillo, M. Satta, D. Catone, A. Giardini, A. Filippi and M. Speranza, *Chem. Commun.*, 2002, 2438.
4 D. Scuderi, A. Paladini, S. Piccirillo, M. Satta, D. Catone, A. Giardini, A. Filippi and M. Speranza, *Phys. Chem. Chem. Phys.*, 2003, **5**, 4570.
5 F. Lahmani, K. Le Barbu and A. Zehnacker-Rentien, *J. Phys. Chem. A*, 1999, **103**, 1991.
6 F. Lahmani, K. Le Barbu-Debus, N. Seurre and A. Zehnacker-Rentien, *Chem. Phys. Lett.*, 2003, **357**, 636.
7 K. Le Barbu, F. Lahmani and A. Zehnacker-Rentien, *J. Phys. Chem. A*, 2002, **106**, 6271.
8 N. Seurre, K. Le Barbu-Debus, F. Lahmani, A. Zehnacker-Rentien and J. Sepiol, *J. Mol. Struct.*, 2004, **692**, 127.
9 M. Shauer, K. S. Law and E. R. Bernstein, *J. Chem. Phys.*, 1985, **82**, 736.
10 J. Yao, H. S. Im, M. Foltini and E. R. Bernstein, *J. Phys. Chem. A*, 2000, **104**, 6197.
11 R. J. Graham, R. T. Kroemer, M. Mons, E. G. Robertson, L. C. Snoek and J. P. Simons, *J. Phys. Chem. A*, 1999, **103**, 9706.
12 N. A. Macleod and J. P. Simons, *Phys. Chem. Chem. Phys.*, 2004, **6**, 2878.
13 J. P. Simons, *et al.*, *J. Phys. Chem. A*, 2001, **105**, 544.
14 M. Mons, E. G. Robertson and P. J. Simons, *J. Phys. Chem. A*, 2000, **104**, 1430.
15 D. Consalvo, A. Van der Avoird, S. Piccirillo, M. Coreno, A. Giardini Guidoni, A. Mele and M. Snels, *J. Chem. Phys.*, 1993, **99**, 8398.
16 T. M. Di Palma, A. Latini, M. Satta, M. Varvesi and A. Giardini Guidoni, *Chem. Phys. Lett.*, 1998, **284**, 184.
17 M. J. Frisch, G. W. Trucks, H. B. Schlegel, G. E. Scuseria, M. A. Robb, J. R. Cheeseman, V. G. Zakrzewski, J. A. Montgomery, Jr., R. E. Stratmann, J. C. Burant, S. Dapprich, J. M. Millam, A. D. Daniels, K. N. Kudin, M. C. Strain, O. Farkas, J. Tomasi, V. Barone, M. Cossi, R. Cammi, B. Mennucci, C. Pomelli, C. Adamo, S. Clifford, J. Ochterski, G. A. Petersson, P. Y. Ayala, Q. Cui, K. Morokuma, D. K. Malick, A. D. Rabuck, K. Raghavachari, J. B. Foresman, J. Cioslowski, J. V. Ortiz, A. G. Baboul, B. B. Stefanov, G. Liu, A. Liashenko, P. Piskorz, I. Komaromi, R. Gomperts, R. L. Martin, D. J. Fox, T. Keith, M. A. Al-Laham, C. Y. Peng, A. Nanayakkara, C. Gonzalez, M. Challacombe, P. M. W. Gill, B. G. Johnson, W. Chen, M. W. Wong, J. L. Andres, M. Head-Gordon, E. S. Replogle and J. A. Pople, *GAUSSIAN 98 (Revision A.6)*, Gaussian, Inc., Pittsburgh, PA, 1998.
18 M. Satta, A. Latini, S. Piccirillo, T. M. Di Palma, D. Scuderi, A. Giardini and M. Speranza, *Chem. Phys. Lett.*, 2000, **316**, 94.
19 D. Scuderi, A. Paladini, S. Piccirillo, M. Satta, D. Catone, A. Giardini, A. Filippi and M. Speranza, *Phys. Chem. Chem. Phys.*, 2002, **4**, 2806.
20 S. Piccirillo, F. Rondino, D. Catone, A. Giardini, Guidoni, A. Paladini, M. Tacconi, M. Satta and M. Speranza, *J. Phys. Chem. A*, 2005, **109**, 1828.
21 D. E. Powers and R. E. Smalley, *J. Chem. Phys.*, 1980, **72**, 5039.
22 S. Piccirillo, M. Satta, D. Catone, D. Scuderi, A. Paladini, F. Rondino, M. Speranza, A. Giardini and Guidoni, *Phys. Chem. Chem. Phys.*, 2004, **10**, 2858.
23 D. Catone, A. Giardini Guidoni, A. Paladini, S. Piccirillo, F. Rondino, M. Satta, D. Scuderi and M. Speranza, *Angew. Chem., Int. Ed.*, 2004, **43**, 1868.
24 A. Filippi, A. Giardini, S. Piccirillo and M. Speranza, *Int. J. Mass Spectrom.*, 2000, **198**, 137.